The High Amplitude δ Scuti Star AD Canis Minoris

Roy Andrew Axelsen
P. O. Box 706, Kenmore, Queensland 4069, Australia; reaxelsen@gmail.com

Tim Napier-Munn
49 Limosa Street, Bellbowrie, Queensland 4070, Australia

Received July 26, 2016; revised September 13, 2016 and October 14, 2016; accepted October 14, 2016

Abstract The high amplitude δ Scuti star AD Canis Minoris was studied by photoelectric photometry (PEP) during one night in February 2011 and by digital single lens reflex (DSLR) photometry during seven nights in January and February 2016. Nine light curve peaks were captured, eight of them by DSLR photometry. A review of the literature enabled us to tabulate 109 times of maximum since 1959, to which we added 9 times of maximum from our data, thus creating the largest dataset to date for this star. Assuming a linear ephemeris, the period of AD CMi was calculated to be 0.122974511 (±0.000000004) d, almost identical to that quoted in earlier literature. We constructed an observed minus computed (O–C) diagram which exhibited a quasi-sinusoidal shape, and fitted a weighted model characterized by combined quadratic and trigonometric functions. The fit indicates that the shape of the O–C diagram is attributable to the effects of a slow increase in the pulsation period of AD CMi at a constant rate, modulated by the light time effect of a binary system. These results confirm those of previous authors, and update most of the coefficients of the equation for the fitted model. The values of all of the coefficients in the function are statistically significant. The rate of increase in the pulsation period of AD CMi was calculated from the entire dataset to be $dP/dt = 6.17 (\pm 0.75) \times 10^{-9}$ d yr^{-1} or $dP/Pdt = 5.01 (\pm 0.61) \times 10^{-8}$ yr^{-1}.

1. Introduction

The variability of AD Canis Minoris was first reported by Hoffmeister in 1934 (quoted by Abhyankar 1959). The period of the star is approximately 0.12297 d (Abhyankar 1959; Anderson and McNamara 1960; Epstein and Abraham de Epstein 1973; Breger 1975), with the most precise period of 0.12297443 d reported up to that time by Breger (1975). O–C (observed minus computed) diagrams constructed from observations obtained from 1959 to 1992 revealed that the data were best described by a quadratic function, which indicated that the period was increasing at a slow constant rate (Jiang 1987 quoted by Rodríguez *et al.* 1988, 1990; Yang *et al.* 1992; Burchi *et al.* 1993). Subsequent O–C diagrams which included more recent observations revealed that the data were best fitted by combined quadratic and trigonometric functions, attributed to a slow constant increase in the period, modulated by the light time effect of a binary system (Fu and Jiang 1996; Fu 2000; Hurta *et al.* 2007; Khokhuntod *et al.* 2007). The period of the orbit of the binary system was variously calculated to be 30 yr (Fu and Jiang 1996), 30.44 yr (Fu 2000), 42.8 yr (Hurta *et al.* 2007), and 27.2 yr (Khokhuntod *et al.* 2007).

Since more than 9 years have elapsed since the last time of maximum (March 2006) published in the table of data for the most recent O–C diagram (Khokhuntod *et al.* 2007), it was decided to perform DSLR photometry of AD CMi, and undertake a detailed review of the literature. These efforts have resulted in an expanded listing of times of maximum from the literature, and the addition of nine new times of maximum from our own observations, one from photoelectric photometry in February 2011, and eight from digital single lens reflex (DSLR) photometry in January and February 2016. In all, this paper analyzes 118 times of maximum, a substantial increase on 81 times of maximum reported by Hurta *et al.* (2007) and 73 reported by Khokhuntod *et al.* (2007).

2. Data and analysis

2.1. Photoelectric photometry

Photoelectric photometry (PEP) was taken with an SSP-5 single channel instrument fitted with a Hamamatsu R6358 multialkali photomultiplier tube, from Optec Inc., Lowell, Michigan. Readings were taken through a Celestron C9.25 Schmidt-Cassegrain telescope on a Losmandy GM8 mount. Three 10-second integrations through a V photometric filter from Optec Inc. were averaged to obtain each observation, with the sequence of targets for each set of observations being: sky, comparison star, variable star, comparison star, sky. The comparison star was TYC 0181 00632 1, with the V magnitude taken to be 8.25. Non-transformed magnitudes in V were calculated since the B–V color indices of the variable and comparison stars (approximately 0.25 and 0.30, respectively) did not differ greatly. Data were collected during several nights, but only on one night in February 2011 were observations from a peak of the light curve obtained.

2.2. DSLR photometry

DSLR photometry was taken with a Canon EOS 500D camera during eight nights in January and February 2016. On two nights, images were obtained through a Celestron C9.25 Schmidt-Cassegrain telescope, and during the other six nights through an Orion ED80mm refracting telescope. A Losmandy GM8 mount was used for both telescopes. Images through the Celestron instrument were taken at 800 ISO with exposures of 120 seconds, and a 15- or 20-second gap between exposures. Images through the Orion instrument were taken at either 400

Table 1. Comparison and check stars for DSLR photometry.

Telescope	*Star*	*Star ID*	*V (V Error)*	*B (B Error)*	*B–V*
80-mm refractor	Comparison	HD 64561	8.25		0.30
	Check	HD 64632	8.52		0.26
235-mm SCT	Comparison	TYC 0181 00560 1	10.072 (0.027)	10.563 (0.039)	0.491
	Check	TYC 0181 00708 1	10.388 (0.021)	10.841 (0.028)	0.453

Notes: V and B–V for the comparison and check stars observed through the 235-mm SCT (Schmidt-Cassegrain telescope) were obtained from APASS (American Association of Variable Star Observers Photometric All Sky Survey (Henden et al. *2015)).*

or 800 ISO, and exposures of 120 or 225 seconds, with a gap of 15 or 30 seconds between exposures. Dark frames were taken during the meridian flip, or at the end of the night's observing run if no meridian flip was made. Flat fields were taken near sunrise the morning after the observations, through a sheet of white acrylic acting as a diffuser placed over the front of the telescope, which was aimed at the zenith.

Comparison and check stars (listed in Table 1) were chosen with B–V color indices as close as possible to those of the variable star. The B and V magnitudes of the comparison and check stars for the images through the Schmidt-Cassegrain instrument were obtained from the AAVSO Photometric All-Sky Survey (APASS; Henden *et al.* 2015), and the color indices calculated from those magnitudes.

Aperture photometry was performed on images from the green and blue channels of the DSLR sensor using the software AIP4WIN (Berry and Burnell 2011), and instrumental magnitudes were calculated. Transformed magnitudes in B and V were determined using transformation coefficients from images of standard stars in the E regions (Menzies *et al.* 1989). The time in JD of each magnitude calculation was taken to be the mid point of each DSLR exposure. The heliocentric correction for each night's data was calculated for the mid point in time of the observing run for the night, and the correction applied to all data points for that night.

2.3. Determination of the times of maximum of the light curves

For PEP, the time of maximum was taken as the time in heliocentric Julian days of the peak value of a fifth-order polynomial function fitted to the data in MICROSOFT EXCEL. The time of maximum was obtained by interpolation after zooming in to the peak of the fitted curve in the spreadsheet. For DSLR photometry the time of maximum for each peak in the light curve was taken as the time of the maximum value of a 10th order polynomial function fitted to the peak, with the polynomial functions calculated by the software PERANSO (Vanmunster 2013).

3. Results

Figures 1 and 2 show light curves of AD CMi from photoelectric photometry and DSLR photometry, respectively, each taken during one night. Photoelectric photometry yielded only one light curve peak. From DSLR photometry, usable light curves were obtained during seven nights of observation, from which eight peaks were captured. The times of maximum of the light curves from DSLR photometry and the errors of the estimates, determined using the software PERANSO, are listed in Table 2. Table 3 lists 118 times of maximum, epochs, and O–C values from the literature and from the observations reported by the present authors. The initial epoch and the initial period used to calculate the epochs and the O–C values were those used by Hurta *et al.* (2007), namely, HJD 2436601.82736 and 0.122974510 d, respectively.

A linear ephemeris calculated from the times of maximum and the epochs listed in Table 3 yielded a period of 0.122974511 (± 0.000000004) d.

We apply to the O–C diagram a model comprising combined quadratic and trigonometric functions, as published by Fu and Jiang (1996), Fu (2000), Hurta *et al.* (2007) and Khokhuntod

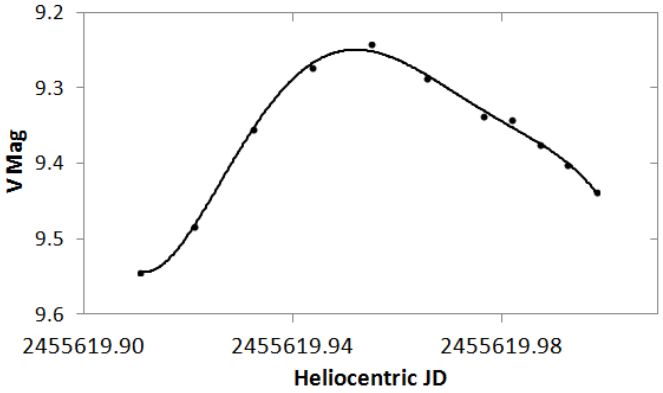

Figure 1. Light curve of AD CMi by photoelectric photometry taken during one night with observations over 2 hours 6 minutes. The solid line is a fifth-order polynomial function, fitted in MICROSOFT EXCEL.

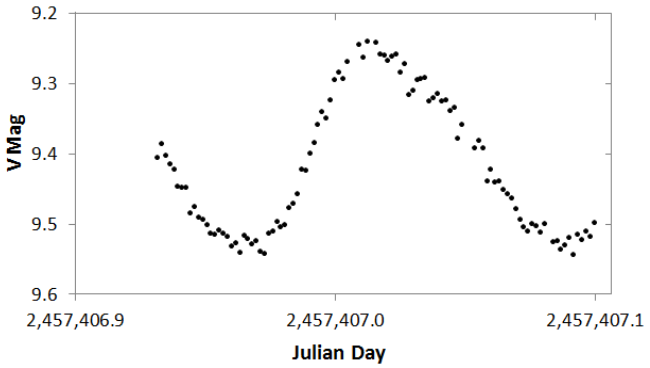

Figure 2. Light curve of AD CMi by DSLR photometry taken during one night with observations over 4 hours 2 minutes.

Table 2. Times of maximum (TOM) in heliocentric Julian days (HJD) of the light curves from DSLR photometry, and the errors of the estimates. The listed values are those output by PERANSO (Vanmunster 2013) , and are not rounded to the last significant digit.

Date	*TOM (HJD)*	*Error*
8-Jan-16	2457396.07261	0.00240
8-Jan-16	2457396.19553	0.00213
11-Jan-16	2457399.02654	0.00171
19-Jan-16	2457407.01750	0.00175
14-Feb-16	2457433.08808	0.00153
15-Feb-16	2457433.95010	0.00182
25-Feb-16	2457444.03359	0.00182
26-Feb-16	2457445.01557	0.00237

et al. (2007). The model implies that the shape of the O–C diagram is attributable to the combined effects of a slow constant rate of increase in the pulsation period of AD CMi, and the light time effect of a stellar pair in mutual orbit.

The model to be fitted is in essence similar to those quoted in the four papers in the previous paragraph, and is represented here in the form:

$$O - C = a + bE + cE^2 + A \sin \phi + B \cos \phi \qquad (1)$$

where E is the epoch (commencing at zero), a, b, c, A, and B are parameters to be estimated from data, and ϕ is the eccentric anomaly, which is the solution to Kepler's equation:

$$\phi - e \sin \phi = 2\pi (1 / P_{orb}) (P_{pul} E - T) \qquad (2)$$

where P_{orb} = orbital period of the pair, P_{pul} = pulsation period of the δ Scuti variable star, T is the time of periastron of the assumed elliptical orbit, and e is the eccentricity of the ellipse. The right-hand side of Equation 2 is the mean anomaly at a given time for a two-body system, M:

$$M = 2\pi (1 / P_{orb}) (P_{pul} E - T) \qquad (3)$$

Kepler's equation (Equation 2) cannot be solved analytically for ϕ and must be solved iteratively. There are several convenient algorithms in the literature. We have used a simple VB macro routine for EXCEL provided by Burnett (1998). This requires three arguments: the mean anomaly, M, the eccentricity, e, and a convergence criterion.

M is easily calculated, given P_{orb}, P_{pul}, and T, for a given epoch, E. Here the values of P_{orb} and T were taken from Hurta et al. (2007) as P_{orb} = 15660 and T = 13870. P_{pul} was assumed to be 0.12297451 day.

For each O–C, E, and ϕ data point, the model of Equation 1 was then fitted by non-linear regression using the MINITAB 16 statistical software package (Minitab 2016). This uses the Gauss-Newton least squares minimization algorithm to estimate the parameters. We did not find the method sensitive to parameter starting values.

Table 4 shows the fitted parameter values, their standard errors, the standard error of the fit, and the P-values for the parameters. The P-values were all statistically significant.

Figure 3 shows the O–C diagram with the predictions of the fitted model and the 95% confidence limits of the model

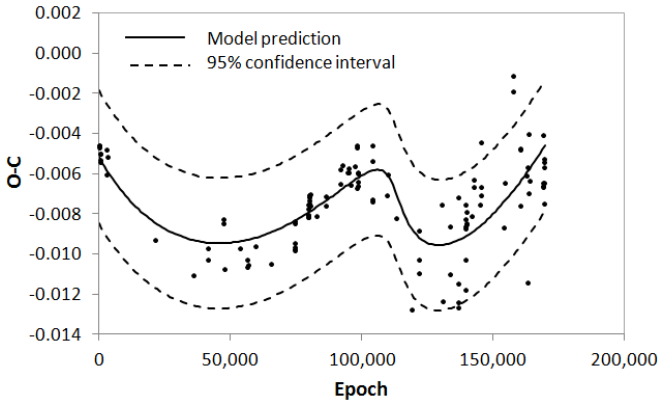

Figure 3. O–C diagram of AD CMi with fitted model prediction (Equation 1) and 95% prediction confidence limits.

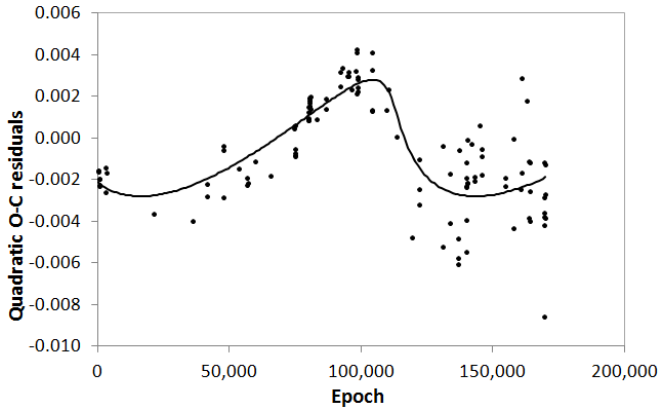

Figure 4. Quadratic residuals for the O–C data of AD CMi, fitted with a function that represents the trigonometric part of Equation 1. The shape of this function reflects the light time effect of the orbital motion of a binary pair.

predictions. The relatively wide confidence intervals reflect the uncertainty in the data and thus the model parameters.

Following Hurta *et al.* (2007), we can show that if the quadratic component of the fitted Equation 1 is subtracted from the original O–C data, the resultant residuals plot has a skewed sinusoidal shape which can then be directly fitted to the sinusoidal component of Equation 1. Thus if we compute $a + bE + cE^2$, where a, b, and c take the values given in Table 3, and subtract these values from the original O–C data, we get the plot shown in Figure 4.

The fitted line in Figure 4 is the function:

$$\text{Residual} = A \sin \phi + B \cos \phi \qquad (4)$$

for the prevailing values of ϕ (and M in Equation 3), fitted by non-linear regression, as before. Equation 4 is the sinusoidal part of Equation 1, and the fitted parameters A and B are identical to those in Table 4. Figure 4 effectively isolates the light time effect of the binary system, and is similar to Figure 2 of Hurta *et al.* (2007), but now extended to include the more recent data. It is worth noting the considerable scatter in the latter part of the plot, which suggests that the model is less well determined for this part of the series (see discussion of weighted regression below).

We can also show that if the trigonometric part of Equation 1 ($A \sin \phi + B \cos \phi$) is subtracted from the original O–C data, the resultant residuals plot has a parabolic shape which can then

Table 3. Data for the O–C diagrams and the key to the references from which the times of maximum (TOM) in heliocentric Julian days (HJD) were taken.

Max	*TOM (HJD)*	*Epoch*	*O–C*	*Reference Key*	*Max*	*TOM (HJD)*	*Epoch*	*O–C*	*Reference Key*
1	2436602.80660	8	–0.0046	1	60	2448714.07240	98494	–0.0063	15
2	2436602.92960	9	–0.0045	1	61	2448717.02420	98518	–0.0059	15
3	2436604.89710	25	–0.0046	1	62	2449399.16250	104065	–0.0072	16
4	2436627.77000	211	–0.0050	1	63	2449399.28820	104066	–0.0045	17
5	2436628.75380	219	–0.0050	1	64	2449400.14620	104073	–0.0073	16
6	2436629.73730	227	–0.0053	1	65	2449401.13200	104081	–0.0053	16
7	2436629.86020	228	–0.0053	1	66	2450071.21840	109530	–0.0070	18
8	2436931.76200	2683	–0.0060	2	67	2450153.36640	110198	–0.0060	19
9	2436932.74700	2691	–0.0048	2	68	2450517.36880	113158	–0.0082	20
10	2436969.76200	2992	–0.0051	2	69	2451268.36960	119265	–0.0127	21
11	2439202.72900	21150	–0.0092	3	70	2451567.07860	121694	–0.0088	5
12	2441010.69850	35852	–0.0110	4	71	2451577.53000	121779	–0.0102	22
13	2441681.52580	41307	–0.0096	5	72	2451598.31200	121948	–0.0109	23
14	2441682.50900	41315	–0.0102	5	73	2452667.57880	130643	–0.0075	5
15	2442429.45800	47389	–0.0084	6	74	2452695.36620	130869	–0.0123	23
16	2442429.45820	47389	–0.0082	7	75	2453028.50550	133578	–0.0110	24
17	2442461.42910	47649	–0.0107	5	76	2453039.57560	133668	–0.0086	5
18	2443182.42970	53512	–0.0096	8	77	2453409.23320	136674	–0.0123	25
19	2443536.34940	56390	–0.0106	8	78	2453411.20050	136690	–0.0126	25
20	2443536.47270	56391	–0.0103	8	79	2453412.18550	136698	–0.0114	25
21	2443572.38100	56683	–0.0105	5	80	2453452.27950	137024	–0.0071	5
22	2443936.26350	59642	–0.0096	5	81	2453776.19280	139658	–0.0087	25
23	2444645.08770	65406	–0.0105	9	82	2453777.05370	139665	–0.0086	25
24	2445766.37130	74524	–0.0084	10	83	2453777.17780	139666	–0.0075	25
25	2445768.33770	74540	–0.0096	10	84	2453781.10870	139698	–0.0118	25
26	2445768.46060	74541	–0.0097	10	85	2453785.04540	139730	–0.0102	25
27	2445771.41340	74565	–0.0083	10	86	2453785.17040	139731	–0.0082	25
28	2445772.39610	74573	–0.0094	10	87	2453810.62589	139938	–0.0085	DKS
29	2445772.51870	74574	–0.0098	10	88	2453810.62591	139938	–0.0084	26
30	2446392.43550	79615	–0.0075	11	89	2453822.55500	140035	–0.0079	5
31	2446417.39910	79818	–0.0077	9	90	2454044.89270	141843	–0.0081	DKS
32	2446418.25960	79825	–0.0080	9	91	2454165.28620	142822	–0.0066	5
33	2446418.38250	79826	–0.0081	9	92	2454172.29610	142879	–0.0063	5
34	2446419.24340	79833	–0.0080	9	93	2454425.86834	144941	–0.0075	DKS
35	2446419.36630	79834	–0.0081	9	94	2454479.36270	145376	–0.0070	27
36	2446443.10100	80027	–0.0075	9	95	2454479.48610	145377	–0.0066	27
37	2446443.22430	80028	–0.0071	9	96	2454515.27390	145668	–0.0044	28
38	2446443.34700	80029	–0.0074	9	97	2455584.53300	154363	–0.0086	29
39	2446444.08500	80035	–0.0073	9	98	2455619.95188	154651	–0.0064	30
40	2446444.20820	80036	–0.0070	9	99	2455997.36600	157720	–0.0011	6
41	2446444.33120	80037	–0.0070	9	100	2455998.34900	157728	–0.0019	6
42	2446493.76700	80439	–0.0070	12	101	2456333.82060	160456	–0.0047	31
43	2446495.73400	80455	–0.0076	12	102	2456346.73010	160561	–0.0076	31
44	2446775.62350	82731	–0.0080	5	103	2456349.68434	160585	–0.0047	HMB
45	2447219.43950	86340	–0.0071	13	104	2456614.93900	162742	–0.0061	31
46	2447220.42280	86348	–0.0075	13	105	2456685.76700	163318	–0.0114	31
47	2447912.27850	91974	–0.0064	11	106	2456699.66888	163431	–0.0056	HMB
48	2447912.40220	91975	–0.0057	11	107	2456726.35600	163648	–0.0040	32
49	2448001.19000	92697	–0.0055	11	108	2456726.47600	163649	–0.0069	32
50	2448254.51710	94757	–0.0059	5	109	2456753.65400	163870	–0.0063	31
51	2448275.29980	94926	–0.0059	11	110	2457396.07261	169094	–0.0065	30
52	2448276.28380	94934	–0.0057	11	111	2457396.19553	169095	–0.0066	30
53	2448406.39000	95992	–0.0065	14	112	2457399.02654	169118	–0.0040	30
54	2448601.42850	97578	–0.0056	11	113	2457407.01750	169183	–0.0064	30
55	2448653.20170	97999	–0.0047	15	114	2457433.08808	169395	–0.0064	30
56	2448656.15110	98023	–0.0067	15	115	2457433.95010	169402	–0.0052	30
57	2448656.27620	98024	–0.0045	15	116	2457444.03359	169484	–0.0056	30
58	2448708.17010	98446	–0.0059	11	117	2457445.01557	169492	–0.0074	30
59	2448713.08840	98486	–0.0066	15	118	2457473.54771	169724	–0.0054	HMB

Notes: The data in the above table were obtained from sources published between 1959 and 2016. The original references are: 1. Abhyankar 1959 (quoted by Rodríguez et al. *1988), 2. Anderson and McNamara 1960, 3. Langford 1976, 4. Epstein and Abraham de Epstein 1973, 5. Hurta* et al. *2007, 6. Paschke 2012b, 7. Breger 1975, 8. Balona and Stobie 1983, 9. Jiang 1987 (quoted by Rodríguez* et al. *1990), 10. Rodríguez* et al. *1988, 11. Kilambi and Rahman 1993 (quoted by Hurta* et al. *2007), 12. Kim and Joner 1994 (quoted by Hurta* et al. *2007), 13. Rodríguez* et al. *1990, 14. Perryman* et al. *1997 (quoted by Hurta al al. 2007), 15. Yang* et al. *1992, 16. Fu* et al. *1996, 17. Hübscher* et al. *1994, 18. Fu 2000, 19. Agerer and Hübscher 1997, 20. Agerer and Hübscher 1998, 21. Agerer and Hübscher 2000, 22. Agerer* et al. *2001, 23. Agerer and Hübscher 2003, 24. Hübscher 2005, 25. Khokhuntod* et al. *2007, 26. Klingenberg* et al. *2006, 27. Hübscher* et al. *2009a, 28. Hübscher* et al. *2009b, 29. Paschke 2012a, 30. Present paper, 31. Pena* et al. *2015, 32. Hübscher and Lehmann 2015. DKS, AAVSO Observer Shawn Dvorak, AAVSO International Database. HMB, AAVSO Observer Franz-Josef Hambsch, AAVSO International Database.*

Table 4. Details of model fit for Equation 1 (unweighted).

Parameter	*Values*	*Standard Errors*	*P-value*
a	-3.02087×10^{-3}	5.62187×10^{-4}	4.20×10^{-7}
b	-1.42480×10^{-7}	1.45067×10^{-8}	7.85×10^{-17}
c	8.49520×10^{-13}	8.24045×10^{-14}	5.76×10^{-18}
A	-2.38332×10^{-3}	2.76352×10^{-4}	4.57×10^{-14}
B	1.47535×10^{-3}	3.15462×10^{-4}	8.13×10^{-6}
Regression std.error	1.60030×10^{-3}		

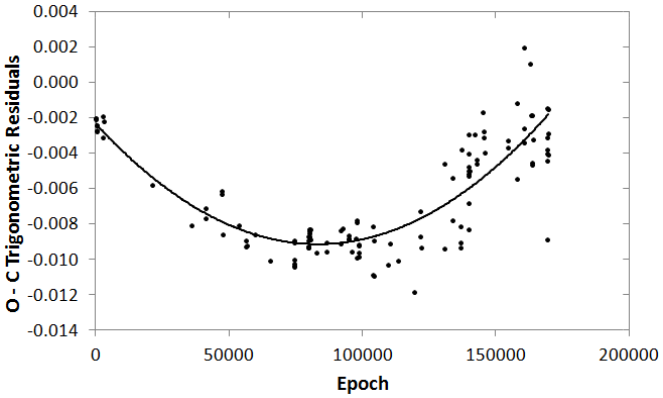

Figure 5. Trigonometric residuals for the O–C data of AD CMi, fitted with a function that represents the quadratic part of Equation 1. The shape of this function indicates the presence of a slow, constant increase in the pulsation period of AD CMi.

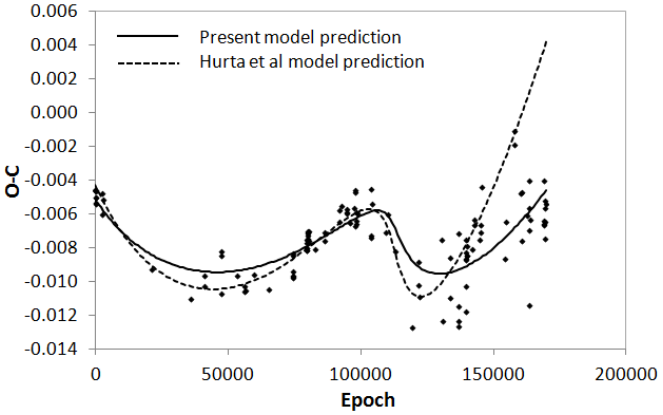

Figure 6. O–C diagram of AD CMi with the model prediction for the present dataset and the earlier dataset from Hurta *et al.* (2007).

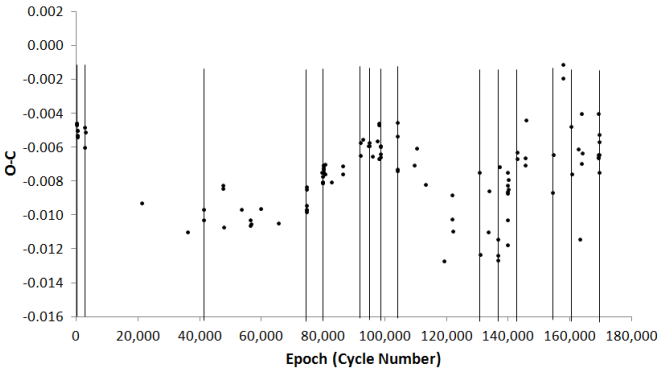

Figure 7. O–C diagram of AD CMi. The vertical lines delineate the groups of O–C values selected for the determination of variance.

be directly fitted to the quadratic component of Equation 1, as shown in Figure 5. This plot effectively isolates the O–C values determined by the pulsation properties of AD CMi. The shape of the O-C diagram and the fitted line (parabolic with concave up) indicates that the period of the star is increasing at a slow steady rate, the value of which is represented by the first differential (equal to 2c) of the second order term (cE^2) of Equation 1.

Figure 6 shows the full dataset again with our model prediction together with that of Hurta *et al.* (2007) as seen in the earlier, less extensive dataset of those authors. It is clear that the two model predictions depart significantly from one another at the later epochs when the new data were collected. The model of Hurta *et al.* is therefore unable to correctly account for the new data.

It is again apparent that the scatter of the data is larger in the later epochs than in the earlier ones. Scatter within a narrow range of epochs reflects experimental error, and is probably mostly due to differences in observers, equipment, and observing conditions. As the scatter varies over the dataset, it would seem sensible to weight the model fitting to reflect this. An appropriate weighting is the inverse of error variance, which can also be described as inverse variance weighting.

An estimate of error variance at a given epoch can be obtained by considering observations taken within any narrow range of epochs as "repeats," and calculating the variance of these to represent the experimental error at the mean epoch of these "repeats." The idea is illustrated in Figure 7, which shows some groupings, comprising the data points on the vertical lines, used to calculate variance.

The range chosen to define "repeats" must be small enough to be able to assume that variations in observational values within this range can be attributed mostly to experimental error and not to true changes in the star's behavior. After careful trial and inspection, 26 groupings of O–C values were found with epoch ranges not exceeding 16 days (the mean was about 9 days), with sample sizes in the range 2–6. We believe the variances of these groups to be attributable principally to observational (experimental) error which can then be used to weight the model fit appropriately.

The variances of the O–C values in these groups are plotted as a function of epoch in Figure 8.

There is a good deal of scatter, probably due to the small sample sizes used to estimate the variance (in the range 2–6), but the linear trend shown is statistically significant (P = 0.00047). Several other models were tried including a quadratic but none gave significantly better fits. Another grouping of data for the calculation of variance was also tried, with a larger number of observations per group, but again the fit was inferior. The equation of the line, which was constrained to pass through the origin, was:

$$\text{Variance} = 6.64 \times 10^{-12}\ \text{Epoch} \qquad (5)$$

This model was used to calculate the variance for each epoch in the original dataset, and the quadratic + sinusoidal model of Equation 1 was then refitted, with weights = 1 / variance. Table 5 shows the new parameters and associated statistics (compare with Table 1 for the unweighted equivalents). Again the P-values

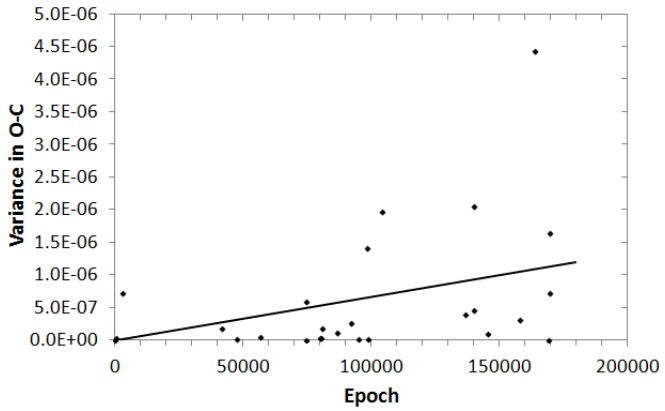

Figure 8. The variances of selected groups of O–C values vs mean epoch data.

Table 5. Details of model fit for Equation (1) (weighted).

Parameter	*Values*	*Standard Errors*	*P-value*
a	-1.98893×10^{-3}	4.84217×10^{-4}	7.60×10^{-5}
b	-1.73831×10^{-7}	2.03459×10^{-8}	6.98×10^{-14}
c	1.03832×10^{-12}	1.26469×10^{-13}	4.01×10^{-13}
A	-2.93094×10^{-3}	4.81185×10^{-4}	1.59×10^{-8}
B	2.01833×10^{-3}	4.32098×10^{-4}	8.32×10^{-6}
Regression std.error	1.64734×10^{-3}		

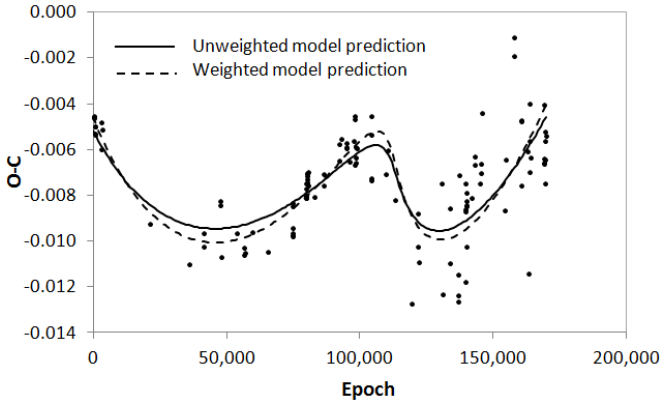

Figure 9. O–C diagram of AD CMi with model predictions for unweighted and weighted data.

show all the parameters to be statistically significant. Figure 9 shows the raw data with the two sets of model predictions, unweighted and weighted.

The two lines are similar but the weighted predictions exhibit higher amplitudes in the cycles. The regression standard errors (controlling prediction uncertainty) are similar (compare Tables 4 and 5).

The rates of change of the pulsation period of AD CMi from the literature and from the observations in the present paper (from the weighted model) are listed in Table 6. Results are included only for those papers which fit a combined quadratic and trigonometric function to the O–C diagram, and are listed in such a manner as to allow easy comparison of the values from the various published sources. It is apparent that there is substantial variation in the values.

4. Discussion

4.1. Issues concerning published times of maximum

Many authors have published data on AD CMi, and several have published tables of epochs and O–C values as well as O–C diagrams (Rodríguez *et al.* 1988, 1990; Yang *et al.* 1992; Fu and Jiang 1996; Hurta *et al.* 2007; Khokhuntod *et al.* 2007). When the literature was reviewed for this paper, a list was made of all published times of maximum, and a comparison of each time of maximum with all other published instances of that time, whether in tables of epochs and O–C values, or as isolated observations. In some cases, the original authors published time series photometry, listing magnitude determinations and the times in heliocentric Julian days or UT of those magnitudes, but did not publish times of maximum of the light curves (Abhyankar 1959; Anderson and McNamara 1960; Epstein and Abraham de Epstein 1973; Balona and Stobie 1983; Kilambi and Rahman 1993). Subsequent papers using those results calculated times of maximum. The present authors chose not to recalculate those times of maximum, instead using the results published by others.

The review of the literature revealed several issues. The first of these relates to the manner in which results published by Anderson and McNamara (1960) are reported by susbsequent authors. Anderson and McNamara reported 38 differential photoelectric observations (delta Y) secured with a yellow filter

Table 6. Rates of change (increase) in the pulsation period of AD CMi.

Reference	*Rate of Period Change* (Error) d cycle^{-13}	*Rate of Period Change* (Error) d yr^{-1}	*Rate of Periot Change* (Error) yr^{-1}
Fu and Jiang 1996	***4.6 × 10^{-13}**	0.14×10^{-8}	1.1×10^{-8}
Fu 2000		***0.10 × 10^{-8}**	*0.81×10^{-8}
Hurta *et al.* 2007		1.15×10^{-8} (0.01×10^{-8})	**9.32×10^{-8} (0.11×10^{-8})**
Khokhuntod *et al.* 2007	**8.6×10^{-13} (0.6×10^{-13})**	0.26×10^{-8} (0.02×10^{-8})	***2.1 × 10^{-8}**
This paper		**0.61×10^{-8} (0.07×10^{-8})**	**5.01×10^{-8} (0.61×10^{-8})**

Notes: These results are only from those papers where combined quadratic and trigonometric functions are fitted to the O–C diagrams. The results for this paper, in the last line of the table, are calculated from the weighted model. Different units were used in various publications, and these are noted at the head of the table. The decimal points are placed in such a way that the numbers in each column can be compared easily. The numbers in bold font represent the coefficients as reported in the original publications, listed in the first column. The numbers not in bold font were calculated by the first author of the present paper, with the aim of presenting all results as d yr^{-1} and yr^{-1} for comparison of the various published values.

** The original authors of these results did not quote estimates of errors.*

relative to the comparison star HD 64275, and listed the UT for each of those observations. The observations captured three peaks of the light curve, as shown in Figure 1 of those authors. However, Rodríguez *et al.* (1990) quote four (not three) times of maximum attributed to Anderson and McNamara, with the first two and the last being identical to the times of maximum listed in Rodríguez *et al.* (1988). It is a mystery why a fourth time of maximum is listed. In addition, the Anderson and McNamara reference is quoted to be *Publ. Astron. Soc. Pacific*, 1961, Vol. 94, p. 289. The year of publication is incorrect (it should be 1960), the volume number for 1961 is actually 72 (not 94), and there is no article beginning on page 289 of the 1961 edition of the journal (according to SAO/NASA ADS). The fourth time of maximum (HJD 2436934.836) attributed to Anderson and McNamara by Rodríguez *et al.* 1990 cannot be confirmed anywhere in the literature by the present authors. It has therefore been omitted from the present paper, although it was reproduced in the tables of times of maximum, epochs, and O–C values by Yang *et al.* (1992), Fu *et al.* (1996), and Khokhuntod *et al.* (2007).

The time of maximum in row 12 of Table 3 above (HJD 2441010.6985 published by Epstein and Abraham de Epstein 1973) is wrongly attributed by Fu *et al.* (1996) to Langford (1976). The time of maximum in row 16 of Table 3 above (HJD 2442429.4582 published by Breger (1975) is wrongly attributed by Fu *et al.* (1996) to Epstein and Abraham de Epstein (1973).

There are two times of maximum in the literature which are times from ephemerides, not directly-observed times of maximum of the peaks of light curves. They are HJD 2436601.8228 (Abhyankar 1959) and HJD 2447506.5815 (Burchi *et al.* 1993). These have therefore been omitted from the O-C table and diagrams in the present paper, although the Abhyankar (1959) time was used by several authors (Rodríguez *et al.* 1988, 1990; Yang *et al.* 1992; Fu *et al.* 1996; Hurta *et al.* 2007; Khokhuntod *et al.* 2007). The Burchi *et al.* (1993) time was used by Hurta *et al.* (2007) and Khokhuntod *et al.* (2007) but both quote it incorrectly as HJD 2447506.5825 (the second last decimal place is incorrect).

The times of maximum in rows 18 to 20 of Table 3 above (i.e., 2443182.4297, 2443536.3494, and 2443536.4727) were calculated from the observations of Balona and Stobie (1983) by Rodríguez *et al.* (1988). The times of maximum corresponding to these and listed by Yang *et al.* (1992), Fu *et al.* (1996), and Khokhuntod *et al.* (2007) are earlier by 0.0004 to 0.0013 HJD.

Kilambi and Rahman (1993) published extensive tables of photometric data on AD CMi, but did not publish times of maximum calculated from those data. Hurta *et al.* (2007) and Khokhuntod *et al.* (2007) calculated and published times of maximum from Kilambi and Rahman's data, and the times of maximum listed by Hurta *et al.* are used in the present paper. The times of maximum in the paper by Khokhuntod *et al.* vary from 0.0054 HJD earlier to 0.0002 HJD later than those of Hurta *et al.* The difference of 0.0054 HJD accounts for one point in the area of wider scatter in O–C values in the O–C diagram of Khokhuntod *et al.* (2007) in comparison with the O–C diagram in the present paper.

Khokhuntod *et al.* (2007) attribute many of the data in their Table 4 to Fu (2000), but that paper does not list any times of maximum for AD CMi. Khokhuntod *et al.* presumably meant to attribute the data to Fu *et al.* 1996. In addition, times of maximum 56 to 58 in Khokhuntod's Table 4 are also attributed to Fu 2000, but were actually first published, respectively, by Agerer and Hübscher (1997, 1998), and Hurta *et al.* (2007).

4.2. Analysis of the O–C diagram

Fu and Jiang (1996), Fu (2000), Hurta *et al.* (2007), and Khokhuntod *et al.* (2007) have indicated that the analysis of the O–C diagram yields a fitted model which can be represented by Equation 1 (repeated from section 3), although the form of the function used by those previous authors differs slightly from that used here:

$$O - C = a + bE + cE^2 + A \sin \phi + B \cos \phi \qquad (1)$$

where ϕ is the solution to Kepler's equation (Equation 2, repeated from section 3):

$$\phi - e \sin \phi = 2\pi \, (1 / P_{orb}) \, (P_{pul} \, E - T) \qquad (2)$$

The function in Equation 1 indicates that the behavior of the O–C diagram is attributable to the combined effects of a slow continuous change (increase) in the pulsation period of AD CMi modulated by the light time effect of a binary pair.

Fu and Jiang (1996), Fu (2000), and Hurta *et al.* (2007) tabulated the coefficients which are the equivalent of a, b, c, A, and B in Equation 1, but Khokhuntod *et al.* (2007) did not. Fu and Jiang (1996), Hurta *et al.* (2007), and Khokhuntod *et al.* (2007) do not describe what method or software was used to derive the fitted model. Fu (2000) indicates that the fit was derived using the software "OMC", referring the reader to a previous publication (Fu *et al.* 1998). We have identified the relevant issue of the journal for that publication, but have not been able to find a copy of the article itself.

We were not able to source software which would analyze the raw O–C data, presumably employing an iterative process or processes, to yield the coefficients a, b, c, A, and B in Equation 1 and simultaneously P_{orb} and T in Equation 2. Therefore, we used the approach outlined above, taking the values of P_{orb} and T (in Equation 2) from Hurta *et al.* (2007) as P_{orb} = 15,660 and T = 13,870. P_{pul} was assumed to be 0.12297451 day. The results from this approach, listed in Table 4, show that the values of the coefficients a, b, c, A, and B are all statistically significant. The model from these coefficients is plotted on the O–C diagram in Figure 3, together with the 95% confidence limits of the model. The quasi-sinusoidal shape of the function is in general similar to those previously published by Hurta *et al.* (2007) and Khokhuntod *et al.* (2007), and supports the modulation of the O–C diagram by the light time effects of a binary system.

The question now arises: does the inclusion of the more recent data in the O–C diagram alter the model? Figure 6 in the present paper indicates that it does. The solid line represents the model from the present paper extending to epoch 169,492, and the dashed line the model of Hurta *et al.* (2007), based on data to epoch 142,879. It can be seen that the model of Hurta *et al.*, when projected into recent epochs, does not predict the more recent data.

It can be seen from the O–C diagrams and Table 3 that the variance of O–C values from epoch 119,265 onwards is greater than the variance of the earlier data. Inspection of the O–C diagram and review of the sources of the more recent data reveal that interobserver variation is the more frequent source of greatest variance, with intraobserver variation contributing, but less frequently. Some observers published only one or two data points near particular epochs, thus preventing an optimal assessment of intraobserver variation in those cases. Given the fact of greater variance in more recent data, it was considered appropriate to weight the model fitting to reflect this. Figure 9 reveals the result. The weighted and unweighted model fitting differ only slightly from one another, the main difference being a greater amplitude of the fitted line as it follows its quasi-sinusoidal course through the data.

The rate of change of the pulsation period of AD CMi is represented by the coefficient (c) of the second order term (cE^2) in the quadratic component of Equation 1, which has the value 1.04 (± 0.13) × 10^{-12} d $cycle^{-1}$. The actual rate is the first derivative of this term, 2c, which has the value 2.08 (± 0.25) ×10^{-12} d $cycle^{-1}$ in the weighted model (Table 5). Converting to the usual units, this value becomes dP / dt = 6.17 (± 0.75) × 10-9 d yr^{-1} or dP / Pdt = 5.01 (± 0.61) × 10^{-8} yr^{-1}. On comparison of these results with previously published rates of increase in the pulsation period of AD CMi, it can be seen (Table 6) that there is substantial variation, with the results from the present paper occupying an intermediate position.

5. Conclusions

We have expanded the O–C diagram of the high amplitude δ Scuti star AD CMi from recent data in the literature and from our own PEP and DSLR photometric observations. Analysis of the O–C diagram has confirmed the work of others that there is a slow constant increase in the pulsational period of the star, modulated by the light time effect of a binary system. We fitted a new, weighted combined quadratic and trigonometric function to the O–C data, based on an orbital period of 42.8 years (Hurta *et al.* 2007), and recalculated the rate of increase in the pulsational period of the δ Scuti star. We note significant variation, in the literature, for the rate of increase in the pulsational period of AD CMi, and for the orbital period of the binary system. Given that the published values for the orbital period vary from 27.2 y (Khokhuntod *et al.* 2007) to 42.8 y (Hurta *et al.* 2007), it may be decades before accurate determinations can be made of the orbital period of the system and the pulsational period of the δ Scuti star.

6. Acknowledgements

We are grateful to AAVSO observers Shawn Dvorak and Franz-Josef Hambsch for their valuable observations from the AAVSO International Database.

The photoelectric photometer used in this study was purchased with a grant from the Edward Corbould Research Fund of the Astronomical Association of Queensland, Brisbane, Australia.

This work utilized data from the AAVSO Photometric All Sky Survey (APASS; Henden *et al.* 2015), funded by the Robert Martin Ayers Sciences Fund.

References

Abhyankar, K. D. 1959, *Astrophys. J.*, **130**, 834.

Agerer, F., Dahm, M., and Hübscher, J. 2001, *Inf. Bull. Var. Stars*, No. 5017, 1.

Agerer, F., and Hübscher, J. 1997, *Inf. Bull. Var. Stars*, No. 4472, 1.

Agerer, F., and Hübscher, J. 1998, *Inf. Bull. Var. Stars*, No. 4562, 1.

Agerer, F., and Hübscher, J. 2000, *Inf. Bull. Var. Stars*, No. 4912, 1.

Agerer, F., and Hübscher, J. 2003, *Inf. Bull. Var. Stars*, No. 5485, 1.

Anderson, L. R., and McNamara, D. H. 1960, *Publ. Astron. Soc. Pacific*, **72**, 506.

Balona, L. A., and Stobie, R. S. 1983, *S. Afr. Astron. Obs. Circ.*, No. 7, 19.

Breger, M. 1975, *Astrophys. J.*, **201**, 653.

Berry, R., and Burnell, J. 2011, "Astronomical Image Processing for Windows," version 2.4.0, provided with *The Handbook of Astronomical Image Processing,* Willmann-Bell, Richmond, VA.

Burchi, R., De Santis, R., Di Paolantonio, A., and Piersimoni, A. M. 1993, *Astron. Astrophys., Suppl. Ser.*, **97**, 827.

Burnett, K. 1998, "Kepler's equation and the Equation of Centre," (http://www.stargazing.net/kepler/kepler.html).

Epstein, I., and Abraham de Epstein, A. E. 1973, *Astron. J.*, **78**, 83.

Fu, J.-N. 2000, in *The Impact of Large-Scale Surveys on Pulsating Star Research*, ed. L. Szabados and D. Kurtz, ASP Conf. Ser. 203, 475.

Fu, J.-N., and Jiang, S.-Y. 1996, *Inf. Bull. Var. Stars*, No. 4325, 1.

Fu, J.-N., Jiang, S.-Y., and Zhou, A.-Y. 1998, *Astrophys. Rep., Publ. Beijing Astron. Obs.*, **32**, 35.

Henden, A. A., *et al.* 2015, AAVSO Photometric All-Sky Survey, data release 9 (http://www.aavso.org/apass).

Hoffmeister, C. 1934, *Astron. Nachr.*, **253**, 195 (quoted by Abhyankar 1959).

Hübscher, J. 2005, *Inf. Bull. Var. Stars*, No. 5643, 1.

Hübscher, J., Agerer, F., Frank, P., and Wunder. E. 1994, *BAV Mitt.*, **68**, 1.

Hübscher, J., and Lehmann, P. B. 2015, *Inf. Bull. Var. Stars*, No. 6149, 1.

Hübscher, J., Steinbach, H.-M., and Walter, F. 2009a, *Inf. Bull. Var. Stars*, No. 5874, 1.

Hübscher, J., Steinbach, H.-M., and Walter, F. 2009b, *Inf. Bull. Var. Stars*, No. 5889, 1.

Hurta, Z., Pócs, M. D., and Szeidl, B. 2007, *Inf. Bull. Var. Stars*, No. 5774, 1.

Jiang, S.-Y. 1987, *Chin. Astron. Astrophys.*, **11**, 343 (quoted by Rodríguez *et al.* 1990).

Khokhuntod, P., Fu, J.-N., Boonyarak, C., Marak, K., Chen, L., and Jiang, S.-Y. 2007, *Chin. J. Astron. Astrophys.*, **7**, 421.

Kilambi, G. C., and Rahman, A. 1993, *Bull. Astron. Soc. India*, **21**, 47.

Kim, C., and Joner, M. D. 1994, *Astrophys. Space Sci.*, **218**, 113 (quoted by Hurta *et al.* 2007).

Klingenberg, G., Dvorak, S. W., and Robertson, C. W. 2006, *Inf. Bull. Var. Stars*, No. 5701, 1.

Langford, W. R. 1976, Ph. thesis, Brigham University (quoted by Rodríguez *et al.* 1990).

Menzies, J. W., Cousins, A. W. J., Banfield, R. M., and Laing, J. D. 1989, *S. Afr. Astron. Obs. Circ.*, No. 13, 1.

Minitab. 2016, MINITAB statistical software (https://www.minitab.com/en-us/).

Paschke, A. 2012a, *Open Eur. J. Var. Stars*, **142**, 1 (http://var.astro.cz/oejv).

Paschke, A. 2012b, *Open Eur. J. Var. Stars*, **147**, 1 (http://var.astro.cz/oejv).

Pena, J. H., *et al.* 2015, *Inf. Bull. Var. Stars*, No. 6154, 1.

Perryman, M. A. C., European Space Agency Space Science Department, and the Hipparcos Science Team. 1997, *The Hipparcos and Tycho Catalogues*, ESA SP-1200 (VizieR On-line Data Catalog: I/239), ESA Publications Division, Noordwijk, The Netherlands (quoted by Hurta *et al.* 2007).

Rodríguez, E., Rolland, A., and López de Coca, P. 1988, *Rev. Mex. Astron. Astrofis.*, **16**, 7.

Rodríguez, E., Rolland, A., and López de Coca, P. 1990, *Inf. Bull. Var. Stars*, No. 3427, 1.

Vanmnuster, T. 2013, light curve and period analysis software PERANSO V.2.50 (http://www.peranso.com/).

Yang, D., Tang, Q., and Jiang, S. 1992, *Inf. Bull. Var. Stars*, No. 3770, 1.